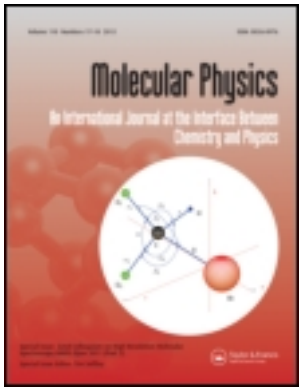

Molecular Physics: An International Journal at the Interface Between Chemistry and Physics
Publication details, including instructions for authors and subscription information:
http://www.tandfonline.com/loi/tmph20

Ionization photophysics and Rydberg spectroscopy of diacetylene

Martin Schwell [a], Yves Bénilan [a], Nicolas Fray [a], Marie-Claire Gazeau [a], Et Es-Sebbar [a], François Gaie-Levrel [b c], Norbert Champion [d] & Sydney Leach [d]

[a] LISA UMR CNRS 7583, Université Paris Est Créteil and Université Paris Diderot, Institut Pierre Simon Laplace, 61 Avenue du Général de Gaulle, 94010, Créteil, France

[b] Synchrotron SOLEIL, L'Orme des Merisiers, St.Aubin, B.P. 48, 91192, Gif-sur-Yvette Cedex, France

[c] Laboratoire national de métrologie et d'essais - LNE (National Metrology Institute and Testing Laboratory), Chemistry and Biology Division, Air Quality and Gaz Flowmetering Department, 1 rue Gaston Boissier, 75724 Paris Cedex 15, France

[d] LERMA UMR CNRS 8112, Observatoire de Paris-Meudon, 5 place Jules-Janssen, 92195, Meudon, France

Accepted author version posted online: 19 Jun 2012.Version of record first published: 11 Jul 2012.

To cite this article: Martin Schwell , Yves Bénilan , Nicolas Fray , Marie-Claire Gazeau , Et Es-Sebbar , François Gaie-Levrel , Norbert Champion & Sydney Leach (2012): Ionization photophysics and Rydberg spectroscopy of diacetylene, Molecular Physics: An International Journal at the Interface Between Chemistry and Physics, 110:21-22, 2843-2856

To link to this article: http://dx.doi.org/10.1080/00268976.2012.704084

Molecular Physics
Vol. 110, Nos. 21–22, November 2012, 2843–2856

Taylor & Francis
Taylor & Francis Group

SPECIAL ISSUE: FASE (FEMTO-, ASTRO-, SPECTRO-ETHYNE)

Ionization photophysics and Rydberg spectroscopy of diacetylene

Martin Schwell[a]*, Yves Bénilan[a], Nicolas Fray[a], Marie-Claire Gazeau[a], Et Es-Sebbar[a]†, François Gaie-Levrel[bc], Norbert Champion[d] and Sydney Leach[d]*

[a]*LISA UMR CNRS 7583, Université Paris Est Créteil and Université Paris Diderot, Institut Pierre Simon Laplace, 61 Avenue du Général de Gaulle, 94010, Créteil, France;* [b]*Synchrotron SOLEIL, L'Orme des Merisiers, St.Aubin, B.P. 48, 91192, Gif-sur-Yvette Cedex, France;* [c]*Laboratoire national de métrologie et d'essais - LNE (National Metrology Institute and Testing Laboratory), Chemistry and Biology Division, Air Quality and Gaz Flowmetering Department, 1 rue Gaston Boissier, 75724 Paris Cedex 15, France;* [d]*LERMA UMR CNRS 8112, Observatoire de Paris-Meudon, 5 place Jules-Jansen, 92195, Meudon, France*

(*Received 7 May 2012; final version received 12 June 2012*)

Photoionization of diacetylene was studied using synchrotron radiation over the range 8–24 eV, with photoelectron-photoion coincidence (PEPICO) and threshold photoelectron–photoion coincidence (TPEPICO) techniques. Mass spectra, ion yields, total and partial ionization cross-sections were measured. The adiabatic ionization energy of diacetylene was determined as $IE_{ad} = (10.17 \pm 0.01)$ eV, and the appearance energy of the principal fragment ion C_4H^+ as $AE = (16.15 \pm 0.03)$ eV. Calculated appearance energies of other fragment ions were used to infer aspects of dissociation pathways forming the weaker fragment ions C_4^+, C_3H^+, C_3^+ and C_2H^+. Structured autoionization features observed in the PEPICO spectrum of diacetylene in the 11–13 eV region were assigned to vibrational components of three new Rydberg series, R1($ns\sigma_g$, n = 4–11), R2($nd\sigma_g$, n = 4–7) and R3($nd\delta_g$, n = 4–6) converging to the $A^2\Pi_u$ state of the cation, and to a new series R′1($ns\sigma_g$, n = 3) converging to the $B'^2\Sigma_u^+$ state of the cation. The autoionization mechanisms and their consistence with specific selection rules are discussed.

1. Introduction

Diacetylene is a molecule whose many physical and chemical aspects in both neutral and ionic forms have inspired interest in fields as varied as absorption and emission spectroscopy, astrophysics, soot formation and biomimetic structures. In many instances photochemistry and photophysics of diacetylene are involved, requiring prior detailed information on its spectroscopy from the far IR to the vacuum ultraviolet. In the Solar System diacetylene has been detected in the atmosphere of Titan, initially observed by infrared spectroscopy in the Voyager 1981 flight [1]. Indeed diacetylene is believed to play an important role in the formation of polyynes and other hydrocarbons in this atmosphere. Since it absorbs at longer UV wavelengths than other major constituents of Titan's atmosphere, it can act as a spectral filter for the larger hydrocarbons formed, thus protecting them from photochemical destruction. Diacetylene has also been seen in the atmospheres of the planets Saturn, Jupiter, Uranus and Neptune [2]. Very recently it has been detected on the moon in an impact experiment [3]. Spectroscopic observations in the interstellar medium (ISM) have shown the presence of diacetylene in the Protoplanetary nebulae CRL 618 and CRL 2688 [4]. Furthermore, the diacetylene cation $C_4H_2^+$ has recently been proposed by Krełowski [5] to be the carrier of a Diffuse Interstellar Band at 5069 A on the basis of matching laboratory spectra and optical absorption spectra observed in translucent interstellar clouds.

Diacetylene plays a role in soot formation, especially in acetylene flames, and in general in combustion processes [6]. It is also a possible intermediate in dust formation in technological plasmas [7]. Photopolymerisation processes involving diacetylene, which polymerizes with 254 nm radiation, have been used to create polymeric diacetylene thin films for nonlinear optical applications based on their third-order nonlinear optical properties [8]. Diacetylene lipid bilayers have been photopolymerized for applications to the fabrication of micropatterned biomimetic membranes [9]. There are many applications of diacetylene in nanotechnology, in particular in the preparation of nanostructures [10].

The present work concerns aspects of the VUV photophysics and photochemistry of diacetylene in the photon excitation range 8 to 24 eV. In particular it bears on dissociative ionization processes and on the

*Corresponding authors. Email: Martin.Schwell@lisa.u-pec.fr; Sydney.Leach@obspm.fr
† Present address: King Abdullah University of Science and Technology, Saudi Arabia

ISSN 0026–8976 print/ISSN 1362–3028 online

http://dx.doi.org/10.1080/00268976.2012.704084
http://www.tandfonline.com

discovery of new Rydberg series of neutral diacetylene in autoionization regions above the ionization limit, studied by photoelectron–photoion conincidence (PEPICO) and threshold photoelectron–photoion coincidence (TPEPICO) methods. Our measurements enabled us to determine total and partial ionization cross-sections which will be of use for astrophysical modelling involving the formation and destruction of diacetylene and its ions.

2. Experimental

Measurements were performed at the undulator beamline DESIRS of the synchrotron radiation (SR) facility Soleil (St. Aubin, France). This beamline incorporates a 6.65 m normal incidence monochromator which is equipped with four different gratings. For our measurements, we used the 200 grooves/mm grating which provides a constant linear dispersion of 7.2 Å/mm at the exit slit of the monochromator. The typical slit width used in our experiments is 100 μm, yielding a monochromator resolution of 0.7 Å under these conditions (about 6 meV at $h\nu = 10$ eV and 18 meV at $h\nu = 18$ eV).

The VUV output of this monochromator can be directed towards two branches. One of them is connected to the permanent end station SAPHIRS which we use. SAPHIRS consists of a molecular beam inlet and an electron-ion coincidence spectrometer called DELICIOUS II. The latter has been described recently in detail [11]. A brief description is given here: The monochromatised SR beam (200 μm horizontal × 100 μm vertical extension) is focused into the ion source of DELICIOUS II which combines velocity map imaging (VMI) of the photoelectrons with a linear time-of-flight mass analyzer operating according to Wiley–MacLaren space focusing conditions. From the electron images, zero kinetic energy electrons can be selected in order to measure Threshold-PEPICO (TPEPICO) mass spectra with resolutions as good as 1 meV. In TPEPICO energy scans, the total resolution is given by convolution of the monochromator resolution and the energy resolution of the threshold electrons. The latter can be chosen *a posteriori* by changing the size of the central area of the VMI image used for the coincidence measurement within an interval depending on the selected extraction field (cf. [11] for more details). In PEPICO scans the spectral resolution is defined only by the slit widths of the monochromator (see above). All photoion yield curves were normalized with respect to the incoming photon flux, continuously measured by a photodiode (AXUV100, IRD).

Here, we present results from two different beamtime periods. In period 1 we chose an effective repeller voltage of $V_{rep} = 500$ V. Under these conditions, only photoelectrons with kinetic energies below $KE_{max} = 0.95$ eV are detected and therefore taken into account for the coincidence measurements. TPEPICO spectra can be recorded with high resolution. After examination of the published photoelectron spectrum of C_4H_2 [12], we chose $V_{rep} = 3000$ V, yielding $KE_{max} = 5.7$ eV in beamtime period 2, in order to be sure that all photoelectrons produced in the 10 to 24 eV energy region are detected by the two-dimensional position sensitive detector of DELICOUS II. Only under these conditions, the PEPICO photoion yield curves are linearly proportional to the ionization cross sections of C_4H_2. We also remark that the TOF mass spectrometer has about 100% transmission efficiency, independent of mass, so that the observed relative PEPICO intensities reflect true branching ratios of dissociative ionization reaction (at high KE_{max}). However, TPEPICO measurements cannot be performed at such high V_{rep}. Finally we note that in our experiment the ions have about 3.5 keV kinetic energy when impinging on the MCP detector so that the mass dependence of the MCP sensitivity can be neglected (cf. ref. [13]).

The beamline is equipped with a gas filter which effectively removes all the high harmonics generated by the undulator that could be transmitted by the grating, thus providing high spectral purity. In this work argon was used as a filter gas for all measurements below 15.75 eV. At higher energies, no filter gas is employed. Lines of the rare gas used in the filter occur in the spectra and are used to calibrate the energy scale to an absolute precision of about 1 meV. In this work, also absorption lines of molecular nitrogen above 16 eV were used to calibrate the energy scale.

We remark that PEPICO fragment ion appearance energies (AEs) correspond to *effective* thermochemical energy values. The two main factors for the possible difference between the measured AE and the 0 K value are: (i) the limited detection sensitivity and (ii) the thermal energy stored in the parent neutral. Fragmentation dynamics (possible activation barriers, formation of vibrationally excited fragments) also influence the effective AE. This has been discussed in more detail earlier by Gaie-Levrel *et al*. [14]. In the present molecular beam experiment, the expected low temperature (~40 K) should, however, provide a value closer to the AE_{0K} than room temperature experiments. Also, compensatory effects may lead to appearance energies that reflect reasonably well their 0 K values as has been pointed out by Chupka [15].

Diacetylene was prepared by dehydrochlorination of 1,4-dichloro-2-butyne ($C_4H_4Cl_2$) in tetraethylene diethyl ether to which a 40% aqueous sodium hydroxide solution was slowly added [16]. Once formed, the compound was carried away in a stream of nitrogen, dried over calcium chloride and was trapped with an acetone/liquid nitrogen slush (−25 to −30°C). It was then distilled at −70°C in order to eliminate impurities. The C_4H_2 purity was monitored by infrared spectroscopy.

C_4H_2 is gaseous at ambient temperature (T_{amb}). In order to avoid its polymerisation, it should however only be stored at low pressure and/or diluted with a rare gas at T_{amb}. For our measurements, the gas is let into a 1 litre stainless steel recipient to attain a pressure $p(C_4H_2) = 50$ mbar. Helium is added to yield a total pressure of $p_{TOT} \approx 3$ bar. This recipient is directly connected to the molecular beam inlet of SAPHIRS using a pressure reducing regulator. Stagnation pressure in SAPHIRS was such that no van der Waals aggregates were formed in the molecular beam. This was checked with the mass spectrometer.

During beamtime period 2, C_4H_2 was further mixed with propane (C_3H_8) as a standard at equal pressure $p(C_4H_2) = p(C_3H_8) = 50$ mbar, in order to measure absolute ionization cross-sections according to the comparative method described by Cool *et al.* [17]. Also here, helium was added to yield a total pressure of $p_{TOT} = 3$ bar. The pressure was measured with a Baratron (MKS). The absolute error of this pressure transducer is estimated to be about ±3%.

3. Results and discussion

3.1. *The photoion mass spectra*

The mass spectra of diacetylene were recorded at a series of photon excitation energies E_{exc} between 11 and 24 eV (Figures 1 and 2). We remark that in our photoion mass spectra each peak exhibits a tail towards longer times-of-flight. This is due to the effects of an inhomogeneous electric field under VMI extraction conditions.

At $E_{exc} = 11$ eV the ions observed are the parent ion *m/z* 50 ($C_4H_2^+$) and *m/z* 51 ($^{13}C^{12}C_3H_2^+$) (figure 1). The latter has a peak intensity that is 5% of that at *m/z* 50. This is the same isotope intensity ratio as in the NIST electron impact mass spectrum (EIMS) [18]. As the excitation energy increases, at 13 eV, in addition to the parent ion, impurities O_2^+ (*m/z* 32, <5% of parent ion intensity, not shown) and H_2O^+ (*m/z* 18) are also observed, the corresponding known ionization energies being 12.07 eV (O_2) and 12.62 eV (H_2O) [18]. The mass spectra at $E_{exc} = 14$ and 15 eV show no new features

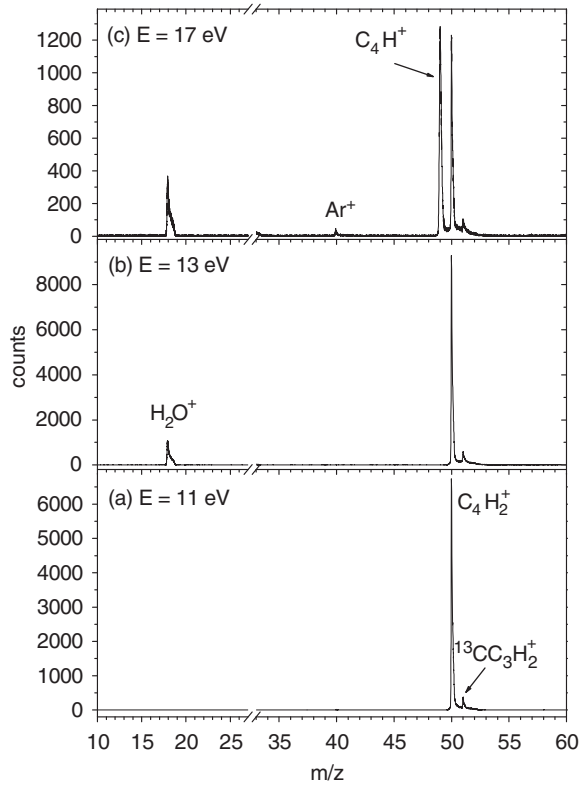

Figure 1. Photoion mass spectra of diacetylene. (a) E = 11 eV, (b) E = 13 eV, (c) E = 17 eV. DELICIOUS II conditions: $KE_{max} = 0.95$ eV.

but at $E_{exc} = 16$ eV a N_2^+ impurity (*m/z* 28) and, very weak, Ar^+ (*m/z* 40) appear (not shown). Their respective ionization energies are 15.58 eV (N_2) and 15.76 eV (Ar) [18]. A new ion appears at $E_{exc} = 17$ eV (see figure 1c). This is C_4H^+ (*m/z* 49), whose appearance energy, determined from its ion yield curve (see below) is $AE = (16.15 \pm 0.03)$ eV. The OH^+ ion (*m/z* 17) is observed at $E_{exc} = 19$ eV (Figure 2a). This is certainly a dissociative ionization product of H_2O; its known appearance energy is 18.12 eV [18].

No measurements were made at $E_{exc} = 20$ eV but at $E_{exc} = 21$ eV there now appear extremely weak signals at *m/z* 16 and *m/z* 48 (Figure 2b). The *m/z* 16 ion is O^+ and results from the dissociative ionization of the impurities O_2 ($AE(O^+) = 18.73$ eV [18]) and/or H_2O ($AE(O^+) = 19$ eV [18]). The *m/z* 48 ion we assign to C_4^+, resulting from dissociative ionization of C_4H_2, as discussed below. At $E_{exc} = 23$ eV (Figure 2c) the *m/z* 48 ion has become more evident while very weak new signals are observed at *m/z* 25 (C_2H^+) and *m/z* 37 (C_3H^+), both being dissociative ionization products of diacetylene, as discussed below. These new signals are reinforced in intensity as E_{exc} increases to 24 eV (Figure 2d).

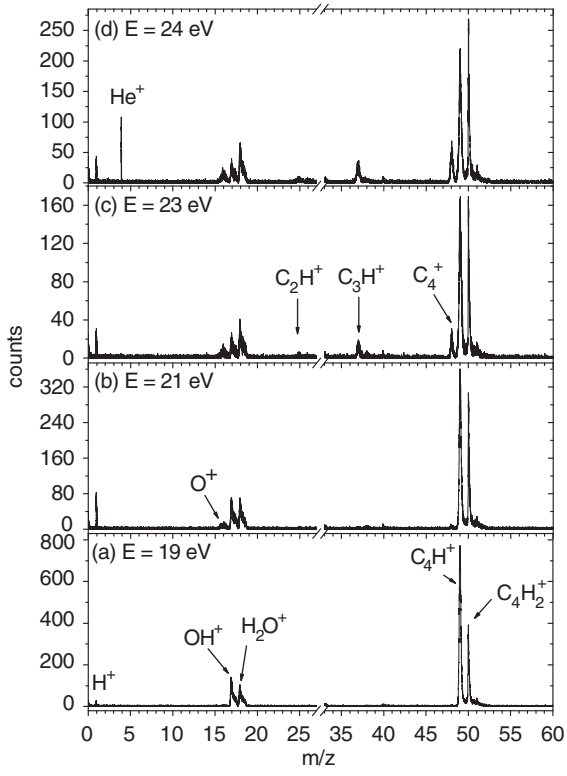

Figure 2. Photoion mass spectra of diacetylene. (a) E = 19 eV, (b) E = 21 eV, (c) E = 23 eV, E = 24 eV. DELICOUS II conditions: $KE_{max} = 0.95$ eV.

We note that the 70 eV EIMS [18] exhibits peaks at m/z 50 (and 51) ($C_4H_2^+$), 49 (C_4H^+), 48 (C_4^+), 37(C_3H^+), 36(C_3^+), 25(C_2H^+), 24(C_2^+), 13(CH^+) and 12(C^+) (see below, Section 4, for a discussion of the fragment ions).

3.2. *Electronic and geometric structural preliminaries*

The presentation and discussion of our PEPICO and TEPEPICO spectra involves the electronic configurations and geometries of the neutral molecule ground state $X^1\Sigma_g^+$ and the ground $X^2\Pi_g$ and three electronic excited states, $A^2\Pi_u$, $B^2\Pi_u$, and $B'^2\Sigma_u^+$ of the diacetylene cation. The relevant data are given below.

The X, A and B' states of the centrosymmetric diacetylene ion are linear and so belong to the $D_{\infty h}$ symmetry group as does the ground state of the neutral species. Rydberg states of diacetylene converging to the X, A and B' ion states will also be linear. The $B^2\Pi_u$ state has been considered as being linear [19].

We first present the electronic configurations of neutral diacetylene and those of the ground and relevant excited electronic states of the cation. Geometric structure data (r_s) of the $X^2\Pi_g$ and $A^2\Pi_u$ ion states [20] are also given, and ionization energies are noted. Electron configurations follow those given by Smith [21] and by Kohima *et al*. [22]. They differ in the relative energies of the $5\sigma_g$ and $4\sigma_u$ molecular orbitals, predicted to be close together, from that given by Bieri and Äsbrink [12], and based on HAM/3 calculations. Our electron configuration also follows that of CO_2, which has the same number and types of molecular orbitals as does diacetylene [23]. We mention that the ion electronic state at 13.865 eV, observed as the upper state of an absorption spectrum of C_4H_2 in a Ne matrix at 3.69 eV [24], does not appear as a HeI photoelectron band [12] and so is most probably the doubly excited $+1\pi_g \rightarrow 2\pi_u$ $B^2\Pi_u$ state [19]. No experimental structural data are known for this state or for the $B'^2\Sigma_u^+$ ion state.

C_4H_2 : ....$5\sigma_g^4\ 4\sigma_u^4\ 1\pi_u^4\ 1\pi_g^4$ $X^1\Sigma_g^+$:

$r_s(C-H) = 1.046$ A, $r_s(C\equiv C) = 1.205$ A,

$r_s(C-C) = 1.376$ A;

$C_4H_2^+$: ....$5\pi_g^4\ 4\sigma_u^4\ 1\pi_u^4\ 1\pi_g^3$ $X^2\Pi_g$:

IE = $82064 \pm 30\ cm^{-1} = 10.175 \pm 0.004$ eV [25]

$r_s(C-H) = 1.046$ A, $r_s(C\equiv C) = 1.234$ A,

$r_s(C-C) = 1.376$ A;

$C_4H_2^+$: ....$5\sigma_g^4\ 4\sigma_u^4\ 1\pi_g^3\ 1\pi_g^4$ $A^2\Pi_u$:

IE = $101787 \pm 30\ cm^{-1} = 12.620 \pm 0.004$ eV

(see below), $r_s(C-H) = 1.045$ A;

$r_s(C\equiv C) = 1.243$ A, $r_s(C-C) = 1.410$ A;

$C_4H_2^+$: ....$5\sigma_g^4\ 4\sigma_u^4\ 1\pi_g^4\ 1\pi_g^2\ 2\pi_u$ $B^2\Pi_u$:

IE = $111828\ cm^{-1} = 13.865$ eV [19, 24]

$C_4H_2^+$: ....$5\sigma_g^4\ 4\sigma_u^3\ 1\pi_g^4\ 1\pi_g^4$ $B'^2\Sigma_u^+$:

IE = $133968 \pm 30\ cm^{-1} = 16.61$ [26]

Although the geometry of this state is not known, we expect the $B'^2\Sigma_u^+$ state to be linear, as an application of Walsh's rules on the bonding properties of the electrons in this configuration [27].

Quartet states of the diacetylene cation are calculated to lie higher than the $A^2\Pi_u$ state although approaching the latter to within $\approx 2000\ cm^{-1}$ as the ion bends [22].

Most of our observed spectral features pertain to ionization forming the $X^2\Pi_g$ state or to Rydberg bands converging to the $A^2\Pi_u$ ion state. In addition, a few bands have been provisionally assigned as n = 3

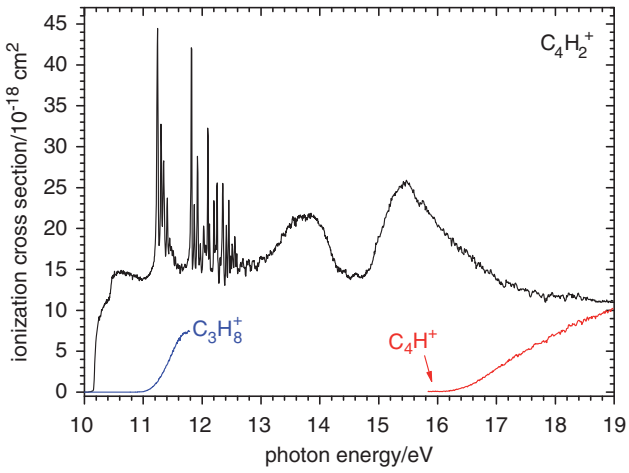

Figure 3. PEPICO ion yield spectra of the diacetylene parent cation $C_4H_2^+$ (m/z 50, black line), the parent cation of propane $C_3H_8^+$ (m/z 44, blue line), and the diacetylene fragment ion C_4H^+ (m/z 49, red line) in the 10–19 eV range. Spectral resolution 1 Å (8.5 meV at 10.3 eV). Propane is used as a standard permitting the conversion of the relative ion yield into absolute ionization cross-section (see text). DELICIOUS II conditions: $KE_{max} = 5.7$ eV.

members of a Rydberg series that converges to the excited electronic state $B'^2\Sigma_u^+$ of the cation.

The modifications in geometry on loss of an electron indicate that the $1\pi_g$ molecular orbital is bonding in C≡C, antibonding in C–C, while the $1\pi_u$ molecular orbital is antibonding in C≡C, bonding in C–C. In view of the large relative energies of the highest occupied π and σ molecular orbitals, diacetylene represents an excellent case of π/σ separation, which lessens possible ambiguities in spectral analysis, in contrast to molecules such as formamide where the proximity of π and σ orbitals renders the spectroscopic and photophysical dynamics complex [28].

3.3. *PEPICO and TPEPICO spectra of diacetylene: analysis and assignments*

The TPEPICO curves were recorded with a total spectral resolution of 20 meV and the PEPICO with a spectral resolution of 8.5 meV at $E_{exc} = 10.3$ eV. PEPICO spectra of the parent ion were measured in the interval 10–19 eV (Figure 3). A series of peaks were observed in the 10–13 eV region. At higher energies the spectra showed few structural features apart from broad bands whose maxima are at 13.6 eV and 15.5 eV. During beamtime period 1 TPEPICO spectra of the parent ion were measured in selected spectral regions (not shown). We first examine the PEPICO and TPEPICO spectra in the 10–10.7 eV region.

3.3.1. *The 10 - 10.7 eV spectral region: diacetylene ion $X^2\Pi_g$ ground state*

Figure 4 shows the PEPICO and TPEPICO spectra of diacetylene in the 10.0 to 10.7 eV region. The adiabatic ionization energy determined from a semi-log representation of the PEPICO curve is IE(C_4H_2) = (10.17 ± 0.01) eV. It is in good agreement with the most accurate published values, (10.180 ± 0.003) eV obtained from Rydberg series in a VUV absorption spectrum [21], and (10.175 ± 0.004) eV [25] from photoelectron spectra in a one-photon resonant, two-photon ionization study of jet-cooled diacetylene via a number of vibronic levels of the 1 $^1\Delta_u$ state. The vertical ionization energy, given by the first strong spectral peak in the TPEPICO spectrum is $IE_{vert} = (10.19 \pm 0.01)$ eV, which is 110 meV less than the value, IE(vert) = 10.30 eV, reported by Bieri and Åsbrink in their He II PES study [12] (no error is given in ref. [12], spectral resolution 60–100 meV). However, from examination of their C_4H_2 PES figure, we estimate a lower IE_{vert}, more in agreement with our value.

Other literature values of the ionization energy of diacetylene are mainly from photoelectron spectra [18]. Turner *et al.* report $IE_{ad} = 10.17$ eV from a HeI PES [29]. Reeher *et al.* [30] measured the ionization energy of the neutral diacetylene fragment formed by electron impact on a series of aromatic molecules and report values over the range IE = 10.08–10.40 eV [30]. The electron impact mass spectrum value of Coats and Anderson is IE = (10.2 ± 0.1) eV [31]. Cool *et al.* [17] in a photoionization cross-section study of diacetylene [16] (measurement steps of 50 meV) mention IE = 10.17 eV, presumably from literature values. We remark that the standard Herzberg book on polyatomic molecules [23] gives an incorrect IE(C_4H_2) = 10.79 eV, based on the early Price and Walsh Rydberg analysis [32].

The heat of formation of diacetylene is reported as 4.81 eV [6,18]. From our IE (C_4H_2) = 10.17 eV we determine $\Delta_f H$ ($C_4H_2^+$) = 14.98 eV. The value in the compilation of Lias et is 14.74 eV [33], but this is based on an earlier value of $\Delta_f H$ (C_4H_2) = 4.56 eV.

The second strong peak in the TPEPICO spectrum is at 10.46 eV and we assign this to excitation of the $\nu_2 = 2178\ cm^{-1}$ vibration in the $X^2\Pi_g$ ground state. This vibrational frequency is very close to that observed in the A-X emission spectrum for the $X^2\Pi_g$ ground state in both the gas phase, $\nu_2 = 2176.6\ cm^{-1}$ [34] and in a Ne matrix spectrum $\nu_2 = 2176\ cm^{-1}$ [35].

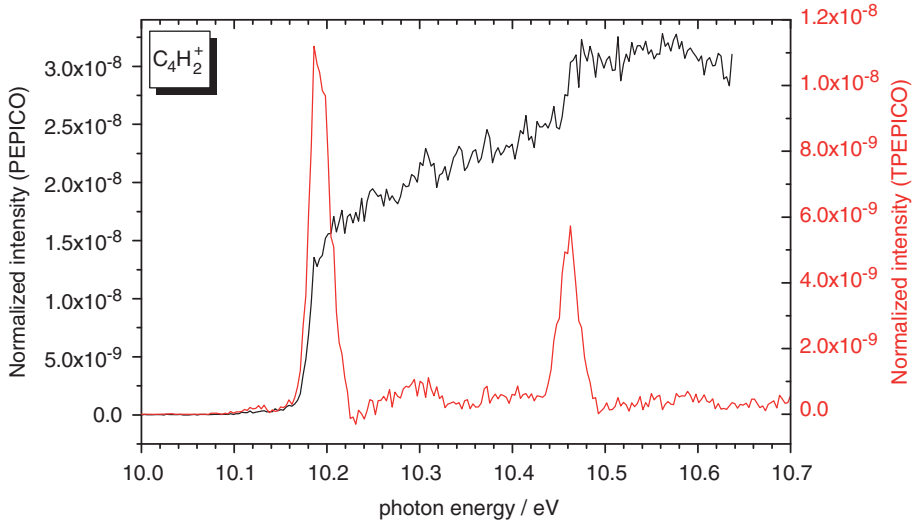

Figure 4. Black line: PEPICO ion yield spectrum, 1 Å spectral resolution (8.5 meV at 10.3 eV). Red line: TPEPICO ion yield spectrum (20 meV total resolution). Step width is 3 meV in both spectra. DELICOUS II conditions: $KE_{max} = 0.95$ eV.

The excitation of this C≡C vibrational mode is consistent with the important lengthening of the C≡C bond, $r_s(C{\equiv}C) = 1.205\,\text{Å} \rightarrow 1.243\,\text{Å}$ in going from the neutral ground state to the cation ground state [20]. This vibronic excitation can also be associated with the step in the PEPICO spectrum at the same energy 10.46 eV (cf. Figure 4).

A weak broad peak at ≈10.3 eV is also observed in the TPEPICO spectrum (Figure 4), separated by ≈110 meV (887 cm^{-1}) from the first peak. This can be assigned to the unresolved Fermi resonance dyad $\nu_3 = 861\,cm^{-1}$ and $2\nu_7 = 972\,cm^{-1}$ [34] excited in the $X^2\Pi_g$ ground state of the ion. Excitation of the triad $2\nu_3 = 1719\,cm^{-1}$, (0.213 eV), $\nu_3 + 2\nu_7 = 1847\,cm^{-1}$ (0.229 eV) and $4\nu_7 = 1958\,cm^{-1}$ (0.243 eV) is possibly responsible for the very weak signal in the 10.37–10.43 eV region.

We mention also a very weak hot band at ≈10.125 eV in the PEPICO spectrum, at about $500 \pm 100\,cm^{-1}$ below the vertical IE. This may correspond to neutral ground state excitation of $2\nu_9 = 440\,cm^{-1}$ ($2 \times 220\,cm^{-1}$) [36]. From the relative intensity of the hot band to that of the $X^2\Pi_g$ 0° band, and using this vibrational frequency, the Maxwell–Boltzmann distribution of diacetylene molecules corresponds to a vibrational temperature in the beam of ≈135 K.

3.3.2. *The PEPICO 11–13 eV spectral region: Rydberg features and assignments*

A considerable number of structured features were observed in the PEPICO spectrum of diacetylene in the 11–13 eV region (Figure 5). These have not been observed before and are principally assigned to three new Rydberg series, R1 (n = 4–11), R2 (n = 4–7) and R3 (n = 4–6), which converge to the first electronic excited state of the diacetylene cation, $A^2\Pi_u$. As mentioned above, there are also four features that are assignable to n = 3 Rydberg bands converging to the $B'^2\Sigma_u^+$ state of the cation.

Vibrational components were observed for each of the Rydberg series. The energies (eV), frequencies (cm^{-1}) and assignments of each feature are given in Table 1. Quantum defects δ, based on the ionization energy 12.62 eV at the Rydberg series limit, are indicated in Table 2 for the origin bands 0_0^0 of each member n of the Rydberg series. Three of these features have been observed previously between 11 and 11.5 eV by Cool *et al.* [17], but in a low resolution photoionization cross section measurement carried out at 40 meV band width (50 meV intervals). The spectrum of Cool *et al.* [17] is undersampled and therefore its intensity ratios are probably incorrect.

Quantum defects were determined using the standard relation: $T(n) = I - R/(n-\delta)^2$, where T(n) is the energy of the spectral term whose principal quantum number is n, the Rydberg constant R = 13.606 eV, and I = 12.62 eV is the energy of the $A^2\Pi_u$ state of the diacetylene ion and I = 16.61 eV for the $B'^2\Sigma_u$ state.

Series limits: The energy of the R1, R2 and R3 series limit, $(101787 \pm 30)\,cm^{-1}$ ((12.620 ± 0.004) eV) is known from the sum of two accurate measurements, which are the $X^2\Pi_g$ ionization energy $802064 \pm 30\,cm^{-1}$ ((10.175 ± 0.004) eV) [25] and the $A^2\Pi_u - X^2\Pi_g$ transition energy of the ion, $T_0 = 19722.61\,cm^{-1}$

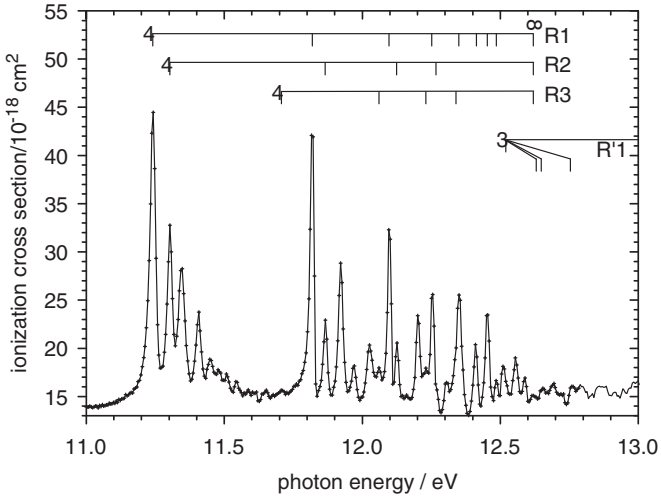

Figure 5. PEPICO ion yield spectrum of $C_4H_2^+$ (m/z 50) in the 11 to 13 eV range (black line; crosses indicate measurement points). Spectral resolution 1 Å. Step width is 5 meV. DELICIOUS II conditions: $KE_{max} = 5.7$ eV. We indicate origin bands of Rydberg series R1, R2 and R3 and vibronic bands for R′1.

(2.4453 eV) [20]. The Ω 1/2 − 3/2 doublet splitting of the $A^2\Pi_u$ state is about 33 cm^{-1} [20] so that the distinction of separate series converging to each of these doublet limits would be lost at our spectral resolution. In view of the relative broadness of the observed bands we chose to work with the known value of the energy of the $A^2\Pi_u$ state as the series limit rather than determine this limit from the observed Rydberg band frequencies. The series limit for Rydberg bands converging to the $B'^2\Sigma_u$ state was taken as the reported adiabatic ionization energy, 16.61 eV of this state [26].

Vibrational analysis: The principal vibrational interval observed is of the order of 830 cm^{-1} in both the R1 and R2 series, and it is ≈800 cm^{-1} in R3, which has few members of this vibrational progression. We consider the first member of the vibrational progressions to be a Fermi resonance dyad between $\nu_3 = 807$ cm^{-1}and $2\nu_7 = 861$ cm^{-1}. The frequencies of these two Fermi resonance components in the $A^2\Pi_u$ state have been determined from fluorescence excitation spectra of the diacetylene ion in a Ne matrix at 4 K [35] in which these dyads are excited. Our value of 830 cm^{-1} corresponds to the unresolved mean of these two features.

In similar fashion, the interval of the order of 1660–1670 cm^{-1} in the R1 and R2 series corresponds to the triad $2\nu_3$, $\nu_3 + 2\nu_7$, $4\nu_7$, also seen in the fluorescence excitation spectra of the diacetylene ion [35]. This Fermi resonance between $2\nu_3 = 1601$ cm^{-1}, (0.198 eV), $\nu_3 + 2\nu_7 = 1671$ cm^{-1} (0.207 eV) and $4\nu_7 = 1752$ cm^{-1} (0.217 eV) has 0.207 eV as the average triad vibrational interval which exactly what is seen in our PEPICO spectrum. In the principal Rydberg series observed, there are also present higher order polyads at additional intervals of ≈830 cm^{-1}. Irregularities in the vibrational intervals in the progressions can result from band profile overlaps of transitions involving Fermi resonance displacement effects and possible Renner–Teller effects in the $A^2\Pi_u$ state. Our spectral resolution is insufficient to further refine the vibrational analysis.

A few bands were observed that are tentatively assigned to the vibration $\nu_2 \approx (1935 \pm 15)$ cm^{-1}. The Ne matrix excitation spectrum value is $\nu_2 = 2002$ cm^{-1}, but examination of the relevant Figure 4 in the paper of Bondybey and English [35] fails to convince one of this particular assignment. We note that HeI photoelectron spectral data [26] provide values $\nu_2 = (1860 \pm 40)$ cm^{-1}, $\nu_3 = (810 \pm 40)$ cm^{-1}.

The excitation of ν_3, which is essentially a central C–C stretch vibration, is consistent with the increase of 0.034 Å in the C–C bond length in going from the neutral molecule to the $A^2\Pi_u$ ion state, insofar as the geometries of the Rydberg states mimic that of the ion state. The comparable corresponding increase in the C≡C bond length, 0.038 Å, does not show up as an important progression in the ν_2 vibration, since only a few bands were (tentatively) assigned to excitation of this vibrational mode. The ν_2 vibration is reported as appearing in the $A^2\Pi_u$ band of He I photoelectron spectra, but appears to be only a minor component from the spectrum published by Turner *et al*. [29], in contrast to the PES $X^2\Pi_g$ band, where it forms a strong progression, even though the C≡C bond length increase is only 0.029 Å in this case. The fact that the C–C bond length *decreases* in going from the neutral ground state to the $X^2\Pi_g$ ion state but *increases* in

Table 1. Rydberg series in the PEPICO spectrum of Diacetylene: Autoionization features and assignments[a].

E/eV	E/cm^{-1}	Assignment	Vibrational frequencies/cm^{-1} [b]
11.239	90,648	4R1 0_0^0	
11.300	91,140	4R2 0_0^0	
11.342	91,479	4R1 3_0^1, 7_0^2	4R1: $\nu_3 = 831$; $2\nu_7 = 831$ (416)
11.404	91,979	4R2 3_0^1, 7_0^2	4R2: $\nu_3 = 839$; $2\nu_7 = 839$ (420)
11.446	92,318	4R1 3_0^2, 3_0^1 7_0^2,7_0^4	4R1: $2\nu_3 = 1670$ (835); $4\nu_7 = 1670$ (418)
11.477	92,568	4R1 2_0^1	4R1:$\nu_2 = 1920$
11.506	92,802	4R2 3_0^2, 3_0^1 7_0^2,7_0^4	4R2: $2\nu_3 = 1662$ (831); $4\nu_7 = 1662$ (416)
11.542	93,092	4R2 2_0^1	4R2: $\nu_2 = 1952$
11.552	93,173	4R1 3_0^3	4R1: $3\nu_3 = 2525$ (842)
11.585	93,439	4R1 2_0^1, 3_0^1 7_0^2	4R1: $\nu_2 = 1960$
11.650	93,963	4R1 3_0^4	4R1: $4\nu_3 = 3315$ (829)
11.707	94,423	4R3 0_0^0	
11.752	94,786	4R1 3_0^5	4R1: $5\nu_3 = 4138$ (828)
11.817	95,310	5R1 0_0^0	
11.865	95,697	5R2 0_0^0	
11.920	96,141	5R1 3_0^1, 7_0^2	5R1: $\nu_3 = 831$; $2\nu_7 = 831$ (416)
11.967	96,520	5R2 3_0^1, 7_0^2	5R2: $\nu_3 = 823$; $2\nu_7 = 823$ (412)
12.025	96,988	5R1 3_0^2, 3_0^1 7_0^2,7_0^4	5R1: $2\nu_3 = 1678$ (839); $4\nu_7 = 1678$ (420)
12.061	97,278	5R3 0_0^0	
12.097	97,568	6R1 0_0^0	
12.124	97,786	5R1 3_0^3	5R1: $3\nu_3 = 2476$ (825)
		6R2 0_0^0	
12.160	98,076	5R3 3_0^1, 7_0^2	5R3: $\nu_3 = 798$; $2\nu_7 = 798$ (399)
12.202	98,415	6R1 3_0^1, 7_0^2	6R1: $\nu_3 = 847$; $2\nu_7 = 847$ (424)
12.230	98,641	6R2 3_0^1, 7_0^2	6R2: $\nu_3 = 855$; $2\nu_7 = 855$ (428)
		6R3 0_0^0	
12.252	98,818	7R1 0_0^0	
12.267 sh[c]	98,939	7R2 0_0^0	
12.306	99,354	6R1 3_0^2, 3_0^1 7_0^2,7_0^4	6R1: $2\nu_3 = 1686$ (843); $4\nu_7 = 1686$ (423)
12.339 sh	99,520	6R2 3_0^2, 3_0^1 7_0^2,7_0^4	6R2: $2\nu_3 = 1734$ (867); $4\nu_7 = 1734$ (434)
		7R3 0_0^0	
12.350	99,609	8R1 0_0^0;	7R1: $\nu_3 = 791$; $2\nu_7 = 791$ (396)
		7R1 3_0^1, 7_0^2	
12.413	100117	9R1 0_0^0	
12.453	100440	10R1 0_0^0	8R1: $\nu_3 = 831$; $2\nu_7 = 831$ (416)
		8R1 3_0^1, 7_0^2	7R1: $2\nu_3 = 1622$ (811); $4\nu_7 = 1622$ (406)
		7R1 3_0^2, 3_0^1 7_0^2,7_0^4	
12.486	100,706	11R1 0_0^0	
12.510	100,899	9R1 3_0^1, 7_0^2	9R1: $\nu_3 = 782$; $2\nu_7 = 782$ (391)
12.522 sh	100,996	3R′1 0_0^0	
12.556	101,270	8R1 3_0^2, 3_0^1 7_0^2,7_0^4	8R1: $2\nu_3 = 1661$ (831); $4\nu_7 = 1661$ (415)
12.589	101,537	11R1 3_0^1, 7_0^2	11R1: $\nu_3 = 831$; $2\nu_7 = 831$ (416)
12.615	101,746	9R1 3_0^2, 3_0^1 7_0^2,7_0^4	9R1: $2\nu_3 = 1629$ (815); $4\nu_7 = 1629$ (407)
12.630	101,867	3R′1 3_0^1	3R′1: $\nu_3 = 871$
12.648	102,012	3R’ 7_0^2	3R′1: $2\nu_7 = 1016$ (508)
12.656	102,077	8R1 3_0^3	8R1: $3\nu_3 = 2468$ (823);
		10R1 3_0^2, 3_0^1 7_0^2,7_0^4	10R1: $2\nu_3 = 1637$ (819); $4\nu_7 = 1637$ (409)
12.691	102,359	11R1 3_0^2, 3_0^1 7_0^2,7_0^4	11R1:$2\nu_3 = 1653$ (827); $4\nu_7 = 1653$ (413)
12.752	102,851	3R′1 2_0^1	3R′1:$\nu_2 = 1855$

Notes: [a]Rydberg series R1, R2 and R3 converge to the $A^2\Pi_u$ state of of $C_4H_2^+$ at 12.62 eV, and the R′1 series converges to the $B'^2\Sigma_u^+$ state at 16.61 eV (see text).
[b]Single quantum values in brackets.
[c]sh = shoulder.

Table 2. Diacetylene Rydberg states converging to the ion $A^2\Pi_u$ ion state. Quantum defects (δ) for 0° bands : R1 = nsσ_g, R2 = ndσ_g and/or ndπ_g, R3 = ndδ_g.

E/eV	$\tilde{\nu}$ cm^{-1}	Assignment	Δ
R1 Rydberg series: $\delta \approx 0.9$			
11.239	90,648	4R1 0_0^0	0.861
11.817	95,310	5R1 0_0^0	0.884
12.097	97,568	6R1 0_0^0	0.899
12.252	98,818	7R1 0_0^0	0.919
12.350	99609	8R1 0_0^0	0.901
12.413	100,117	9R1 0_0^0	0.893
12.453	100,440	10R1 0_0^0	0.974
12.486	100,706	11R1 0_0^0	0.923
R2 Rydberg series: $\delta \approx 0.77$			
11.300	91,140	4R2 0_0^0	0.789
11.865	95,697	5R2 0_0^0	0.755
12.124	97,786	6R2 0_0^0	0.762
12.267 sh	98,939	7R2 0_0^0	0.792
R3 Rydberg series: $\delta \approx 0.07$ (leaving aside 4R3).			
11.707	94,423	4R3 0_0^0	0.14
12.061	97,278	5R3 0_0^0	0.066
12.230	98,641	6R3 0_0^0	0.093
12.339 sh	99,520	7R3 0_0^0	0.042

going to the $A^2\Pi_u$ state must play a role in modifying the Franck–Condon factors involving excitation of ν_2. Calculation of the corresponding Franck–Condon factors would help to understand the vibronic excitation behaviour, including that of the degenerate ν_7 vibration (symmetric C≡C–C bend) in the vibrational dyads and polyads.

Assignments of the Rydberg series R1, R2 and R3: Optically allowed (dipole) transitions in Hund's case a and b coupling (assumed in the present case) for the Rydberg states converging to the $A^2\Pi_u$ ion state are:

$$\ldots.5\sigma_g^4\ 4\sigma_u^4\ 1\pi_u^4\ 1\pi_g^4\ X^1\Sigma_g^+ \rightarrow 1\pi_u^{-1}\ ns\sigma_g^1\ \ \Pi_u$$
$$\ldots.5\sigma_g^4\ 4\sigma_u^4\ 1\pi_u^4\ 1\pi_g^4\ X^1\Sigma_g^+ \rightarrow 1\pi_u^{-1}\ nd\sigma_g^1\ \ \Pi_u$$
$$\ldots.5\sigma_g^4\ 4\sigma_u^4\ 1\pi_u^4\ 1\pi_g^4\ X^1\Sigma_g^+ \rightarrow 1\pi_u^{-1}\ nd\pi_g^1\ \ \Pi_u$$
$$\ldots.5\sigma_g^4\ 4\sigma_u^4\ 1\pi_u^4\ 1\pi_g^4\ X^1\Sigma_g^+ \rightarrow 1\pi_u^{-1}\ nd\delta_g^1\ \ \Pi_u$$

Thus we expect one s-type Rydberg series (nsσ_g), and three d-type series (ndσ_g, ndπ_g, ndδ_g). We observe what are apparently 3 Rydberg series R1 $\delta \approx 0.9$; R2 $\delta \approx 0.77$; R3 $\delta \approx 0.07$ (except 4R3) (Table 2) and we assign them as follows:

R1 is nsσ_g: $\delta \approx 0.9$. This is a reasonable quantum defect for a highly penetrating nsσ Rydberg series [37].

R2 is ndσ_g or, less probably, ndπ_g: $\delta \approx 0.77$. The value $\delta \approx 0.77$ is reasonable for a ndσ_g assignment in diacetylene since in molecules such as C_2H_2 $\delta = 0.50$ for ndσ_g and in C_2H_4 $\delta = 0.60$ for ndσ_g [37].

R3 is ndδ_g: $\delta \approx 0.07$. The first member of this series, n = 4 is anomalous ($\delta \approx 0.14$) indicating some penetration of the 4 dδ_g Rydberg electron.

We remark that one of the Rydberg series converging to the $X^2\Pi_g$ state of the ion also has a large quantum defect, $\delta = 0.87$, assigned provisionally to an nsσ series [38]. Concerning our R2 series, one alternative assignment is to consider that the R2 Rydbergs could be π^{-1} npσ_u $^1\Pi_u$ and/or π^{-1} npπ_u $^1\Sigma_u^+$. However, these are forbidden transitions, although two analogous forbidden transitions have been reported in CO_2 [39] and whose quantum defects are $\delta = 0.64$ and $\delta = 0.55$ [40]. We note that allowed npσ and npπ Rydberg series in acetylene have quantum defects $\delta = 0.70$ [37].

Assignments of the Rydberg series R′1 The four features at 12.522, 12.630, 12.648 and 12.752 eV respectively (Table 1) could not be fitted into Rydberg series converging to the $A^2\Pi_u$ state. Although they would well fit n = 4 Rydberg levels converging to the $B^2\Pi_u$ state at 13.865 eV, the absence of a corresponding peak for this ion state in the HeI photoelectron spectrum and the double excitation nature of the corresponding Rydberg and ionization transitions make this assignment highly unlikely. We therefore considered whether the features could correspond to Rydberg states converging to the $B'^2\Sigma_u^+$ state, whose adiabatic ionization energy is reported to be 16.61 eV by Baker and Turner [26]. Examination of the published corresponding complex photoelectron band [26] indicates that the uncertainty in determining the adiabatic ionization energy is probably at least 100 meV. Nevertheless, using I = 16.61 eV, the R′1 features could correspond to the origin band and vibronic components of a n = 3 member of a Rydberg series with a quantum defect $\delta = 1.18$. In our provisional assignment of these bands, a quantum defect of this magnitude would correspond to an nsσ series. The vibrational components are $\nu_3 = 871\ cm^{-1}$, $2\nu_7 = 1016\ cm^{-1}$ and $\nu_2 = 1855\ cm^{-1}$ (Table 1).

Finally, we mention that if the ion state at 16.61 eV were a $^2\Sigma_g^+$ state, i.e. there is an inversion of the order of the $4\sigma_u$ and $5\sigma_g$ molecular orbitals in the configuration previously given above, the nsσ_g molecular Rydberg transition would be forbidden, but npσ_u and npπ_u transitions would be allowed, with quantum defects of the order of 0.7 [37]. The $\delta = 1.18$ value which we observe for the R′1 bands indicates that the Rydberg state is indeed $^2\Sigma_u^+$ and not a $^2\Sigma_g^+$ state, i.e. it

confirms the molecular orbital order that we presented earlier.

Autoionization mechanism in the R1, R2, R3 Rydberg states The Rydberg features seen in the PEPICO spectrum result from autoionization processes. In autoionization, in order to satisfy selection rules, the outgoing electron from the Rydberg states converging to the $A^2\Pi_u$ state of the ion must have ungerade symmetry, since the final ion state in the autoionization process, the...$1\pi_u^4\ 1\pi_g^3\ X^2\Pi_g$ state ion core, has gerade symmetry.

We note than in our PEPICO spectrum the R1 Rydberg bands are more intense than the R2 bands as is expected from their relative Rydberg assignments. We remark, however, that Smith reports n = 3, 4 and 5 absorption spectra members of a Rydberg series, at 77976, 91120 and 95696 cm^{-1}, respectively [21], which, for n = 4 and 5, correspond to our 4R2 0_0^0 and 5R2 0_0^0 PEPICO bands at 91140 cm^{-1} and 95697 cm^{-1} respectively (Smith's 77976 cm^{-1} band is below the first ionization energy and therefore not observable in PEPICO experiments). He makes no mention of R1 bands. The latter are either apparently weaker than the R2 bands in the absorption spectrum of diacetylene, which would be in contradiction with their Rydberg assignments, or, more likely, the hydrogen many-line spectral source in Smith's experiment was inadequate to reveal the R1 features [21]. Furthermore, Smith notes that in his spectra there is considerable interference above 11.2 eV due to trace water and oxygen bands, making it difficult to follow the bands in this region. We note also that Cool *et al.* [17], in their photoionization cross section study of diacetylene, report the n = 4 R1 0_0^0 band at a 11.2 eV peak (photoionization cross section 44.82 Mb) and another peak at 11.3 eV, which can be considered to be due, at least in part, to the 4R2 0_0^0 transition, according to our observations (Table 1). In an electron excitation study of the dipole forbidden transitions in diacetylene by Allan [38] there is a small feature at 11.3 eV, but none in the 11.2 eV region (upmost spectrum in Figure 6 of ref. [38]).

It is important to study the relative intensities of the R1 and R2 bands in going from absorption to autoionization in order to determine the relative rates of autoionization of the R1 Rydberg levels with respect to the R2 levels. Calculations of relative transition intensities, and measurement of diacetylene absorption spectra carried out with a true continuum spectral source, and of higher resolution than that of Smith, are necessary in order to more thoroughly investigate the dynamics of the Rydberg state relaxation processes.

Further to the question of the relaxation of the Rydberg levels of diacetylene, we mention the photochemical study of Silva *et al.* [41] at 11.7 eV, using two-photon laser excitation (2×212 nm) via an intermediate $^1\Delta_u$ electronic state of diacetylene. Neutral molecule photodissociation occurs at this energy, the principal dissociation processes being $C_4H_2 + h\nu\ (11.7\,eV) \rightarrow C_4H + H$ and $C_4H_2 + h\nu\ (11.7\,eV) \rightarrow C_2H + C_2H$; the branching ratios are computed to be 68% and 20%, respectively. Silva *et al.* suggest that the intermediate state undergoes electronic relaxation before excitation by the second photon, so that the final excitation level is in the 9–10 eV region. However, it seems more reasonable to us that the final level is indeed at 11.7 eV, which corresponds to excitation to the R3 0_0^0 band $4s\sigma_g$ Rydberg level. A measurement of the photodissociation quantum yield at 11.7 eV would be useful. It must be less than unity since autoionization occurs at that excitation energy and would be in competition with photodissociation.

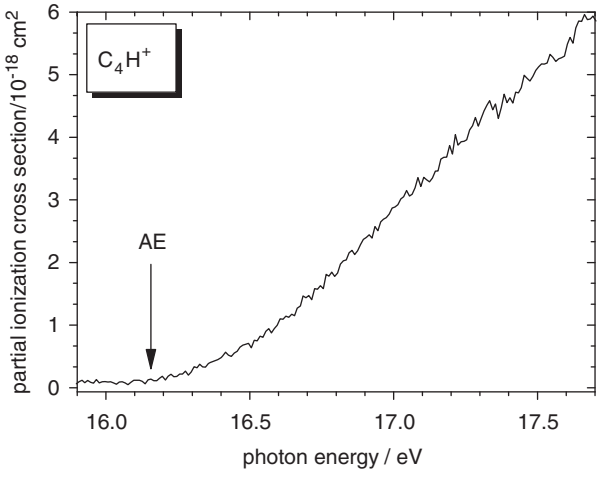

Figure 6. PEPICO ion yield spectrum of C_4H^+ (m/z 49) in the 15.8 to 17.7 eV range. The appearance energy of this fragment is determined to be AE (C_4H^+) = (16.15 ± 0.03) eV. Step width 10 meV. DELICOUS II conditions: $KE_{max} = 5.7$ eV. The partial ionization cross-section of the dissociation channel $C_4H_2^+ \rightarrow C_4H^+ + H$ can be read on the ordinate.

Absolute ionization cross-section of C_4H_2 One aim of our study was to measure absolute ionization cross sections to be used for atmospheric and/or astrophysical modelling. In Figures 3 and 5 we give ionization cross-sections on the ordinate that have been obtained using a comparative method [17] and propane as a standard. The ionization cross section of propane is taken from Kameta *et al.* [42]. We note that, using this standard, our cross section is lower, by a factor of 2, than the only C_4H_2 measurement found in the literature which is from Cool *et al.* [17]. This is consistent

with recent work of Wang *et al*. [43] who measured photoionization cross sections of propane. They find higher values, by a factor of 2 (at 11.5 eV), than Kameta *et al*. [42] but do not discuss this disagreement. The group of Cool rely on propene as a standard and work from the 70 s performed by Person and Nicole [44]. The apparatus of the latter authors was calibrated using photoionization cross sections of nitric oxide measured by Watanabe *et al*. [45] in 1967.

We note that the work of Kameta *et al*. [42] represents an independent measurement since they measure the absolute photoabsorption cross section and the ionization quantum yield of propane in the same experiment and thus do not need any cross-calibration. We therefore tend to rely more on their findings than on those from Cool *et al*. [17,43]. However, this inconsistency in the literature has to be sorted out in the future.

4. Fragment ions

PEPICO ion yield curves were measured only for parent ion (m/z 50) and the C_4H^+ (m/z 49) fragment ion. From our mass spectral data other ions would be too weak or have too high appearance energies for their ion yield curves to be determined.

C_4H^+: Figure 6 gives the PEPICO ion yield curve for m/z 49, assigned to the C_4H^+ fragment ion. In our mass spectra the m/z 49 (C_4H^+) is already of comparable intensity to that of the parent ion at m/z 50 at $E_{exc} = 17$ eV (Figure 1), whereas in the PEPICO ion yield curve the parent ion intensity is about 5 times that of $m/z = 49$ at 17 eV (Figure 3). This is because of the difference of KE_{max} in both measurements. True cross-sections and branching ratios of dissociative photoreactions can only be measured at high KE_{max}. It was carefully checked on the VMI images that, at $KE_{max} = 5.7$ eV, all electrons are captured for the PEPICO measurement.

From Figure 6 we determine the appearance energy of the C_4H^+ ion to be AE (C_4H^+) = (16.15 ± 0.03) eV. Coats and Anderson [31] report an electron impact mass spectrum AE (C_4H^+) = (12.1 ± 0.3) eV, i.e. ≈500 meV below the first excited state $A^2\Pi_u$ of $C_4H_2^+$ which lies at 12.62 eV. However, the $A^2\Pi_u$ state is known to fluoresce, with a lifetime of (71 ± 3) ns for its zero vibrational level [46] and with similar lifetimes for at least 1000 cm^{-1} excitation energy in this state. Thus dissociation of the $A^2\Pi_u$ state would have an extremely small rate, if it occurred, so that we can consider the AE(C_4H^+) = 12.1 eV of Coates and Anderson as incorrect.

The measured AE's can be used to calculate enthalpies of formation of fragment ions m_I^+ (Equation (1)) for different possible fragmentation pathways, using Equation (2):

$$M + h\nu \rightarrow M^+ + e^- \rightarrow m_I^+ + n\, m_i + e^- \qquad (1)$$

$$AE + \Delta_f H_{gas}(M) - \Sigma[\Delta_f H_{gas}(m_i)] = \Delta_f H_{gas}(m_I^+) \qquad (2)$$

Here, m_i are the formed n neutral fragments (including possible isomers). The dissociation ionization process is $C_4H_2 + h\nu \rightarrow C_4H^+ + H$. From our experimental AE(C_4H^+) = (16.15 ± 0.03) eV and using $\Delta_f H(C_4H_2) = 4.81$ eV [6,18] and $\Delta_f H(H) = 2.259$ eV [18] we calculate the heat of formation $\Delta_f H(C_4H^+) = 18.70$ eV (1805 kJ/mol), using Equation (2). This is the first reported value of $\Delta_f H(C_4H^+)$ and should be considered as an upper limit.

We can also estimate the ionization energy of the C_4H radical as follows. Potential energy surface calculations of ground state neutral diacetylene have been carried out at the CCSD(T)/CBS + ZPE(B3LY/6-311 G** level of theory [41]. The dissociation to linear $C_4H + H$ occurs at 5.765 eV above the ground state of diacetylene. From this value and our observed AE(C_4H^+) = 16.15 eV, also assumed to be to a linear ion, we derive IE(C_4H) = 10.39 eV. There is no other value of this ionization energy in the literature.

Other ions seen in mass spectra of diacetylene: It is of interest to use thermochemical data to calculate the expected appearance energies of the other ions seen in the photon impact and/or electron impact mass spectra of diacetylene.

$$m/z\ 48:\ C_4H_2 + h\nu \rightarrow C_4^+ + H + H \text{ or } C_4^+ + H_2$$

The calculated AE(C_4^+) = 22.31 eV for H + H products, and 17.79 eV for the H_2 product channel. Our mass spectra (Figure 2) show that AE(C_4^+) is about 22 eV. This indicates that the dissociation channel is to H + H rather than to H_2 at threshold.

$$m/z\ 37:\ C_4H_2 + h\nu \rightarrow C_3H^+ + CH$$

Using $\Delta_f H(C_3H^+) = 16.58$ eV [47] and $\Delta_f H(CH) = 6.158$ eV [47] we obtain a calculated value AE(C_3H^+) = 17.93 eV for the appearance energy of the 2-propynylidyne radical cation. Our photon impact mass spectra (Figure 2) show that AE(C_3H^+) is between 22 and 23 eV. Thus there is a high barrier to this dissociation. Potential energy surface calculations of the dissociation channel are needed to verify quantitatively this conclusion.

$$m/z\ 36:\ C_4H_2 + h\nu \rightarrow C_3^+ + CH_2$$

From $\Delta_fH(C_3^+) = 20.77\,eV$ [33] and $\Delta_fH(CH_2) = 4.0\,eV$ [47] we calculate $AE(C_3^+) = 19.96\,eV$. In our photon impact mass spectra there is no peak at m/z 36 over the whole range 11–24 eV (Figures 1, 2), showing that the true appearance energy probably lies above 24 eV, thus implying a large potential energy barrier in this dissociative ionization channel.

$$m/z\ 25:\ C_4H_2 + h\nu \rightarrow C_2H^+ + C_2H$$

Two values of $\Delta_fH(C_2H)$ are quoted in the literature, 4.94 eV and 5.76 eV [18]. A calculated value is 5.84 eV [48]. The ionization energy of C_2H is reported as $IE(C_2H) = (11.61 \pm 0.07)\,eV$ [18], so that $\Delta_fH(C_2H^+) = 16.55$ or 17.37 eV. From these values the calculated $AE(C_2H^+) = 16.68$ or 18.32 eV, depending on the value of $\Delta_fH(C_2H)$. Our mass spectra show an extremely weak signal at 22 eV, becoming a little stronger at 23 eV and weakening at 24 eV (Figure 2), indicating a small partial cross section for this dissociative ionization channel. We note that Coats and Anderson [31] report an electron impact mass spectrum appearance energy value for m/z 25, $AE(C_2H^+) = 20.1 \pm 0.5\,eV$, broadly consistent with our photon impact observation that $21\,eV < AE(C_2H^+) < 22\,eV$.

From the calculated neutral dissociation channel to $C_2H + C_2H$ at 6.92 eV above the diacetylene ground state [41] and the known $IE(C_2H) = 11.61 \pm 0.07\,eV$ [18], Equation (2) enables us to calculate another C_2H^+ appearance energy value, $AE\ (C_2H^+) = 18.53\,eV$, which is close to the higher of the two calculated values above.

$$m/z\ 24:\ C_4H_2 + h\nu \rightarrow C_2^+ + C_2H_2$$

From $\Delta_fH(C_2^+) = 20.6\,eV$ [33] and $\Delta_fH(C_2H_2) = 2.35\,eV$ [18] we obtain the calculated value $AE(C_2^+) = 18.4\,eV$. A similar value, $AE(C_2^+) = 18.14\,eV$, is obtained by addition of $IE(C_2) = 12.15\,eV$ [18] to the calculated potential energy value 6.056 eV [41] of the $C_2 + C_2H_2$ dissociation channel of neutral diacetylene. Although C_2^+ is observed very weakly in 70 eV electron impact mass spectra [18], no peak at m/z 24 is noted over the whole range 11–24 eV of our photon impact mass spectra (Figures 1, 2).

$$m/z\ 13:\ C_4H_2 + h\nu \rightarrow CH^+ + C_3H$$

The CH^+ ion is observed very weakly in the 70 eV electron impact mass spectrum [18] but not in our photon impact mass spectra up to $E_{exc} = 24\,eV$ (Figures 1, 2). The AE for this ion could not be estimated since there is no reported value of $\Delta_fH(C_3H)$.

$$m/z\ 12:\ C_4H_2 + h\nu \rightarrow C^+ + C_3H_2$$

The C^+ ion is observed very weakly in the 70 eV electron impact mass spectrum [18] but not in our photon impact mass spectra up to $E_{exc} = 24\,eV$ (Figures 1, 2). The AE for this ion could not be estimated since the value of $\Delta_fH(C_3H_2)$ is not known.

5. Conclusion

Direct and indirect photoionization processes in diacetylene were studied using synchrotron radiation as photon excitation source over the spectral range 8–24 eV, using photoelectron–photoion coincidence (PEPICO) and threshold photoelectron–photoion coincidence (TPEPICO) techniques to determine mass spectra, ion yields, total and partial ionization cross-sections. The adiabatic ionization energy of diacetylene was determined as $IE_{ad} = (10.17 \pm 0.01)\,eV$, in good agreement with optical spectroscopic measurements. An improved heat of formation of the ion, $\Delta_fH(C_4H_2^+) = 14.98\,eV$ was established.

Absolute ionization cross sections of C_4H_2 were determined in the 10 to 19 eV energy regime (Figure 3) using a comparative method and propane as a standard. The ionization cross section of propane is taken from an independent measurement by Kameta *et al.* [42].

The appearance energy of the C_4H^+ photofragment was measured as $(16.15 \pm 0.03)\,eV$ and it was shown that the only previous literature value AE $(C_4H^+) = (12.1 \pm 0.3)\,eV$, of Coates and Anderson [31] is incorrect. The heat of formation of C_4H^+ was determined to be $\Delta_fH(C_4H^+) = 18.70\,eV$ and the formerly unknown ionization energy of C_4H was estimated as $IE(C_4H) = 10.39\,eV$. The partial ionization cross section of the $C_4H_2 + h\nu \rightarrow C_4H^+ + H$ fragmentation channel was measured between the AE of C_4H^+ and 19 eV.

The appearance energies of other fragment ions observed in photon or electron impact ionization of diacetylene, estimated by thermochemical calculations, have led to some inferences concerning the dissociation pathways forming the fragment ions C_4^+, C_3H^+, C_3^+ and C_2H^+.

Autoionization features in the PEPICO and TPEPICO spectra were analysed. The many structured features observed in the PEPICO spectrum of diacetylene in the 11–13 eV region were principally assigned to three Rydberg series, R1 (n = 4–11), R2 (n = 4–7) and R3 (n = 4–6) never previously observed or analysed. These Rydberg series converge to the first electronic excited state of the diacetylene cation, $A^2\Pi_u$. Vibrational components were observed for each of the

Rydberg series and their assignments given. Four other features are assignable to n = 3 vibrational components of an R′1(nsσ_g) Rydberg series converging to the $B'^2\Sigma_u^+$ state of the cation. Quantum defects δ were determined for the origin bands 0_0^0 of each member n of the Rydberg series. The different series converging to the ion $A^2\Pi_u$ state were assigned as follows: R1(nsσ_g), R2(ndσ_g), R3(ndδ_g). The autoionization mechanisms and their conformity with specific selection rules are discussed. The results of this work are used to clarify the nature of the final excited state in the two-photon laser photochemical study of diacetylene by Silva *et al.* [41].

Our mass spectroscopic measurements, thermochemical parameter value estimations, the determination of total and partial ionization cross-sections and the analysis of diacetylene Rydberg series will be of use for astrophysical modelling involving the formation and destruction of diacetylene and its ions in various astrophysical sites.

Acknowledgements

The authors wish to thank Gustavo Garcia and Laurent Nahon for excellent support at the DESIRS beamline as well as the Soleil staff for running the facility.

Reference

[1] V.G. Kunde, A.C. Aikin, R.A. Hanel, D.E. Jennings, W.C. Maguire and R.E. Samuelson, Nature **292**, 686 (1981).
[2] V.S. Meadows, G. Orton, M. Line, M.C. Liang, Y.L. Yung, J. Van Cleve and M.J. Burgdorf, Icarus **197**, 585 (2008).
[3] A. Colaprete, P. Schultz, J. Heldmann, D. Wooden, M. Shirley, K. Ennico, B. Hermalyn, W. Marshall, A. Ricco, R.C. Elphic, D. Goldstein, D. Summy, G.D. Bart, E. Asphaug, D. Korycansky, D. Landis, L. Sollitt, Science **330**, 463 (2011).
[4] J. Cernicharo, A.M. Herras, A.G.G.M. Tielens, J.R. Pardo, F. Herpin, M. Guélin and L.B.F.M. Waters, Ap. J. Lett. **546**, L123 (2001).
[5] J. Krelowski, Y. Beletsky, G.A. Galazutdinov, R. Kołos, M. Gronowski and G. LoCurto, Ap. J. Lett. **714**, L64 (2010).
[6] J.H. Kiefer, S.S. Sidhu, R.D. Kern, K. Xie, H. Chen and L.B. Harding, Combust. Sci and Tech. **82**, 101 (1992).
[7] M. Mao, J. Benedikt, A. Consoli and A. Bogaerts, J. Phys. D **41**, 225201 (2008).
[8] B. Luther-Davies and M. Samoc, Curr. Opinion Solid State Mater. Sci. **2**, 213 (1997).
[9] K. Morikagi, T. Baumgart, U. Jonas, A. Offenhäusser and W. Knoll, Langmuir **18**, 4082 (2002).
[10] T.P. Vinod, J.H. Chang, J. Kim and S.W. Rhee, Bull. Korean Chem. Soc. **29**, 799 (2008).
[11] G.A. Garcia, H. Soldi-Lose and L. Nahon, Rev. Sci. Instr. **80**, 023102 (2009).
[12] G. Bieri and G. Asbrink, J. Electron Spectrosc. **20**, 149 (1980).
[13] J. Oberheide, P. Wilhelms and M. Zimmer, Meas. Sci. Technol. **8**, 351 (1997).
[14] F. Gaie-Levrel, C. Gutlé, H.-W. Jochims, E. Rühl and M. Schwell, J. Phys. Chem. A, **112**, 5138 (2008).
[15] W.A. Chupka, J. Chem. Phys. **30**, 191 (1959).
[16] M. Khlifi, P. Paillous, C. Delpech, M. Nishio, P. Bruston and F. Raulin, J. Mol. Spectrosc. **174**, 116 (1995).
[17] T.A. Cool, J. Wuang, K. Nakajima, C.A. Taatjes and A. Mciiroy, Int. J. Mass Spectrom. **247**, 18 (2005).
[18] NIST Chemistry Webbook (June 2005), National Institute of Standards and Technology Reference Database. Available from http://webbook.nist.gov (current 2009).
[19] J. Zhang, X. Guo and Z. Cao, J. Chem. Phys. **131**, 144307 (2009).
[20] J. Lecoultre, J.P. Maier and M. Rösslein, J. Chem. Phys. **89**, 6081 (1988).
[21] W.L. Smith, Proc. Roy. Soc. Lond. A **300**, 519 (1967).
[22] N. Komiha, P. Rosmus and J.P. Maier, Mol. Phys. **105**, 893 (2007).
[23] G. Herzberg, *Electronic Spectra of Polyatomic Molecules* (Van Nostrand, Princeton, NJ, 1966).
[24] J. Fulara, M. Grutter and J.P. Maier, J. Phys. Chem. A **111**, 11831 (2007).
[25] C. Ramos, P.R. Winter, T.S. Zwier and S.T. Pratt, J. Chem. Phys. **116**, 4011 (2002).
[26] C. Baker and D.W. Turner, Proc. Roy. Soc. Lond. A **308**, 19 (1968).
[27] A.D. Walsh, J. Chem. Soc. 2266 (1953).
[28] S. Leach, H.-W. Jochims and H. Baumgärtel, J. Phys. Chem. **114**, 4847 (2010).
[29] D.W. Turner, C. Baker, A.D. Baker and C.R. Brundle, *Molecular Photoelectron Spectroscopy* (Wiley-Interscience, London, 1970).
[30] J.R. Reeher, G.D. Flesch and H.J. Svec, Org. Mass Spectrom. **11**, 154 (1976).
[31] F.H. Coats and R.C. Anderson, J. Am. Chem. Soc. **79**, 1340 (1957).
[32] W.C. Price and A.D. Walsh, Trans.Faraday Soc. **41**, 381 (1945).
[33] G. Lias, John E. Bartmess, J.F. Libman, J.L. Holmes, R.D. Levin and W.G. Mallard, J. Phys. Chem. Ref. Data **17** (Suppl. No. 1), 872 (1988).
[34] J.H. Callomon, Can. J. Phys. **34**, 1046 (1956).
[35] V.L. Bondybey and J.H. English, J. Chem. Phys. **71**, 777 (1979).
[36] N.L. Owen, C.H. Smith and G.A. Williams, J. Mol. Struct. **161**, 33 (1987).
[37] E. Lindholm, Arkiv Fysik **40**, 97 (1968).
[38] M. Allan, J. Chem. Phys. **80**, 6020 (1984).
[39] Y. Tanaka, A.S. Jura and F.J. LeBlanc, J. Chem. Phys. **32**, 1199 (1960).
[40] E. Lindholm, Arkiv Fysik **40**, 125 (1969).

[41] R. Silva, W.K. Gichuchi, C. Huang, M.B. Doyle, V.V. Kislov, A.M. Mebel and A.G. Suits, Proc. Nat. Acad. Sci. **105**, 12713 (2008).
[42] K. Kameta, N. Kouchi, M. Ukai and Y. Hatano, J. Electron. Spectrosc. Relat. Phenom. **123**, 225 (2002).
[43] J. Wang, B. Yang, T.A. Cool, N. Hansen and T. Kasper, Int. J. Mass Spectrom. **269**, 210 (2008).
[44] J.C. Person and P.P. Nicole, J. Chem. Phys. **53**, 1767 (1970).
[45] K. Watanabe, F.M. Matsunaga and H. Sakai, Appl. Opt. **6**, 391 (1967).
[46] M. Allan, E. Kloster-Jensen and J.P. Maier, Chem. Phys. **7**, 11 (1976).
[47] J.L. Holmes, C. Aubry and P.M. Mayer, *Assigning Structures to Ions in Mass Spectrometry* (CRC Press, Boca Raton, FL, 2007).
[48] R. Janoschek and M.J. Rossi, Int. J. Chem. Kinet. **34**, 550 (2002).